

# Reliability-based analysis of strip footings using response surface methodology

D.S. Youssef Abdel Massih

University of Nantes & Lebanese University, Beirut, Lebanon

A.-H. Soubra

University of Nantes, Institut de Recherche en Génie Civil et Mécanique, UMR CNRS 6183 Bd. de l'Université, BP, Saint-Nazaire Cedex, France

**ABSTRACT:** A reliability-based analysis of a shallow strip foundation is presented. Both the ultimate and the serviceability limit states are considered. Two deterministic models based on numerical simulations are used. The first one computes the ultimate bearing capacity of the foundation and the second one calculates the footing displacement due to a footing applied load. The response surface methodology is utilized for the assessment of the Hasofer-Lind reliability indexes. Only the soil shear strength parameters are considered as random variables while studying the ultimate limit state. Also, the randomness of only the soil elastic properties is taken into account in the serviceability limit state. The assumption of uncorrelated variables was found conservative in comparison to the one of negatively correlated variables. The failure probability of the ultimate limit state was highly influenced by the variability of the angle of internal friction. However, for the serviceability limit state, the accurate determination of the uncertainties of the Young modulus was found very important in obtaining reliable probabilistic results. Finally, the computation of the system failure probability involving both ultimate and serviceability limit states was presented and discussed.

## 1 INTRODUCTION

The commonly used approaches in the analysis and design of shallow foundations are deterministic. Average values of the input parameters are usually considered and the uncertainties of the different parameters are taken into account *via* a global factor of safety which is essentially a 'factor of ignorance'. A reliability-based approach for the analysis of foundations is more rational since it enables to consider the inherent uncertainty of each input parameter. Nowadays, this is possible because of the improvement of our knowledge on the statistical properties of the soil (Phoon and Kulhawy 1999).

In this paper, a reliability-based analysis of a strip foundation resting on a  $c$ - $\varphi$  soil and subjected to a central vertical load is presented. Previous investigations on the reliability analysis of foundations focused on either the ultimate or the serviceability limit state (Fenton & Griffiths 2003; Bauer & Pula 2000 and Youssef Abdel Massih et al. 2007). This paper considers both limit states in the reliability analysis of foundations. Two deterministic models based on the Lagrangian explicit finite difference code  $FLAC^{3D}$  are used. The first one computes the ultimate bearing

capacity of the foundation and the second one calculates the footing displacement due to an applied service load. The response surface methodology is utilized to find an approximation of the analytically-unknown performance functions and the corresponding reliability indexes. The random variables considered in the analysis are the soil shear strength parameters  $c$  and  $\varphi$  for the ultimate limit state and, the soil elastic properties  $E$  and  $\nu$  for the serviceability limit state. After a brief description of the basic concepts of the theory of reliability, the two deterministic models based on numerical  $FLAC^{3D}$  simulations are presented. Then, the probabilistic analysis and the corresponding numerical results are presented and discussed.

## 2 BASIC RELIABILITY CONCEPTS

Two different measures are commonly used in literature to describe the reliability of a structure: The *reliability index* and the *failure probability*. The reliability index of a geotechnical structure is a measure of the safety that takes into account the inherent uncertainties of the input parameters. The widely used

reliability index is the one defined by Hasofer and Lind (1974). Its matrix formulation is given by:

$$\beta_{HL} = \min_{x \in F} \sqrt{(x - \mu)^T C^{-1} (x - \mu)} \quad (1)$$

in which  $x$  is the vector representing the  $n$  random variables,  $\mu$  is the vector of their mean values,  $C$  is their covariance matrix and  $F$  is the failure region. The minimisation of equation (1) is performed subject to the constraint  $G(x) \leq 0$  where the limit state surface  $G(x) = 0$ , separates the  $n$ -dimensional domain of random variables into two regions: a failure region  $F$  represented by  $G(x) \leq 0$  and a safe region given by  $G(x) > 0$ . The classical approach for computing the reliability index  $\beta_{HL}$  by equation (1) is based on the transformation of the limit state surface into the space of standard normal uncorrelated variates. The shortest distance from the transformed failure surface to the origin of the reduced variates is the reliability index  $\beta_{HL}$ . An intuitive interpretation of the reliability index was suggested in Low and Tang (1997) where the concept of an expanding ellipsoid led to a simple method of computing the Hasofer-Lind reliability index in the original space of the random variables. These authors stated that the minimization of the reliability index is equivalent to find the smallest dispersion ellipsoid that is tangent to the limit state surface. When the random variables are non-normal and correlated, the optimisation approach uses the Rackwitz-Fiessler equivalent normal transformation without the need to diagonalize the correlation matrix as shown in Low (2005). The computations of the equivalent normal mean  $\mu^N$  and equivalent normal standard deviation  $\sigma^N$  for each trial design point are automatically found during the constrained optimization search. The method of computation of the reliability index using the concept of an expanding ellipsoid suggested by Low and Tang (1997) is used in this paper. From the First Order Reliability Method *FORM* and the Hasofer-Lind reliability index  $\beta_{HL}$ , one can approximate the failure probability as:

$$P_f \approx \Phi(-\beta_{HL}) \quad (2)$$

where  $\Phi(\cdot)$  is the cumulative distribution function of a standard normal variable.

### 3 DETERMINISTIC NUMERICAL MODELLING OF BEARING CAPACITY AND DISPLACEMENT OF STRIP FOOTINGS

*FLAC<sup>3D</sup>* (Fast Lagrangian Analysis of Continua) is a commercially available three-dimensional finite difference code in which a Lagrangian explicit calculation scheme and a mixed discretization zoning technique are used. It should be mentioned that

*FLAC<sup>3D</sup>* includes an internal programming option (*FISH*) which enables the user to add his own subroutines. In this code, although a static (*i.e.* non-dynamic) mechanical analysis is required, the equations of motion are used. The solution to a static problem is obtained through the damping of a dynamic process by including damping terms that gradually remove the kinetic energy from the system. It should be mentioned that in *FLAC<sup>3D</sup>*, the application of velocities or stresses on a system creates unbalanced forces in this system. Damping is introduced in order to remove these forces or to reduce them to very small values compared to the initial ones. The stresses and deformations are calculated at several small timesteps (called hereafter cycles) until a steady state of static equilibrium or plastic flow is achieved. The convergence to this state may be controlled by a maximal prescribed value of the unbalanced force for all elements of the model.

#### 3.1 Numerical simulations

##### 3.1.1 Ultimate limit state – Bearing capacity

This section focuses on the determination of the ultimate bearing capacity of a rough rigid strip footing, of breadth  $B = 2$  m, resting on a  $c$ - $\phi$  soil and subjected to a vertical load.

Because of symmetry, only half of the entire soil domain of width  $20B$  and depth  $5B$  is considered. The bottom and right vertical boundaries are far enough from the footing and they do not disturb the soil mass in motion (*i.e.* velocity field) for all the soil configurations studied in this paper. A non uniform mesh composed of 904 zones is used. For the half mesh on the right hand side (Figure 1), the region under the footing was divided horizontally into 15 zones, which size gradually decreases from the center to the edge of the footing where very high stress gradients are developed. Beyond the edge of the footing, the domain was divided into 30 zones which size gradually increases from the foundation edge to the right vertical boundary. Vertically, the domain was divided into 20 zones which size decreases gradually from the bottom of the

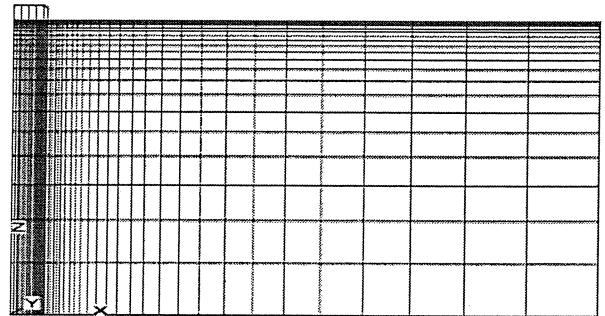


Figure 1. Soil domain and mesh used in *FLAC<sup>3D</sup>*.

domain to the ground surface. Since this is a 2D case, all displacements in the direction parallel to the footing are fixed. For the displacement boundary conditions, the bottom boundary was assumed to be fixed and the vertical boundaries were constrained in motion in the horizontal direction.

A conventional elastic-perfectly plastic model based on the Mohr-Coulomb failure criterion is used to represent the soil. The soil elastic properties used are the shear modulus  $G = 23$  MPa and the bulk modulus  $K = 50$  MPa (for which the equivalent Young's modulus and Poisson's ratio are respectively  $E = 60$  MPa and  $\nu = 0.3$ ). The values of the soil shear strength parameters used in the analysis are:  $\phi = 30^\circ$ ,  $\psi = 20^\circ$  and  $c = 20$  kPa where  $\psi$  is the soil dilation angle. The soil unit weight was taken equal to  $18 \text{ kN/m}^3$ . The strip footing of half width equal to 1 m and depth 0.5 m is simulated by a weightless elastic material. It is divided horizontally into four zones. The footing elastic properties used are the Young's modulus  $E = 25$  GPa and the Poisson's ratio  $\nu = 0.4$ . Compared to the soil elastic properties, these values are well in excess of those of the soil and ensure a rigid behavior of the footing. It was found that the soil and footing elastic properties have a negligible effect on the failure load. The footing is connected to the soil via interface elements that follow Coulomb law. The interface is assumed to have a friction angle equal to the soil angle of internal friction, dilation equal to that of the soil and cohesion equal to the soil cohesion in order to simulate a perfectly rough soil-footing interface. Normal stiffness  $K_n = 10^9$  Pa/m and shear stiffness  $K_s = 10^9$  Pa/m are assigned to this interface. It was found that these parameters do not have a major influence on the failure load.

For the computation of the ultimate bearing capacity of a rigid rough strip footing using *FLAC*<sup>3D</sup>, the following procedure is adopted: Geostatic stresses are first applied to the soil, and then several cycles are run in order to arrive to a steady state of static equilibrium. Finally, the obtained displacements are set to zero in order to obtain the footing displacement due to only the footing load. In a second stage, a controlled downward vertical velocity (*i.e.* displacement per timestep) is applied to the nodes of the footing. Damping of the system is introduced by running several cycles until a steady state of plastic flow is developed in the soil underneath the footing. This state is achieved when both conditions (i) a constant footing load and (ii) small values of unbalanced forces, were satisfied as the number of cycles increases. The number of cycles required to reach this state depends on the value of the applied velocity. At each cycle, the vertical footing load is obtained by using a *FISH* function that calculates the integral of the normal stress components for all elements in contact with the footing. The value of the vertical footing load at the plastic steady state is the ultimate footing load. The ultimate bearing

capacity is then obtained by dividing this load by the footing area.

Several control parameters, such as the intensity of the vertical velocity and the mesh size, may greatly affect the value of the ultimate footing load.

An optimal vertical velocity must be chosen in order to reach a value of the ultimate bearing capacity close to the smallest most critical one (corresponding to very small velocity) with a reasonable computation time. A velocity of  $2.5 \times 10^{-6}$  m/timestep downward was suggested by Yin et al. (2001) as a result of a number of verification runs. This value was tested in the present paper, and an ultimate load of 2393.1 kN/m was obtained at the plastic steady state (for which a continuous increase in the footing vertical displacement is obtained for a constant footing load). A smaller velocity of  $10^{-6}$  m/timestep and a higher velocity of  $5 \times 10^{-6}$  m/timestep were also tested. The value of the ultimate load corresponding to the smaller velocity was found equal to 2392.7 kN/m which is slightly smaller than the one obtained by applying the  $2.5 \times 10^{-6}$  m/timestep velocity. However, an increase in the calculation time by 76% was necessary to reach this value. For the higher velocity of  $5 \times 10^{-6}$  m/timestep, a slightly greater value of 2394.48 kN/m was obtained. The difference is smaller than 0.1% from the value obtained using the  $10^{-6}$  m/timestep velocity with a decrease in the calculation time by 72%. Thus, the  $5 \times 10^{-6}$  m/timestep velocity is adopted in this paper.

The effect of the mesh size on the solution was also checked. It was found that a more refined mesh under the footing does not improve the value of the footing load and may cause numerical instability. A more refined mesh beyond the edge of the footing improves the result (*i.e.* reduces the ultimate load) by only 0.27% with an increase in the calculation time by 36%. Thus, the mesh presented above will be used in all subsequent calculations.

### 3.1.2 Serviceability limit state – vertical displacement

For the computation of the vertical displacement of the footing under an applied load, it would not be interesting to apply uniform stresses directly to the surface nodes of the soil since this approach corresponds to the simulation of a flexible footing. Thus, the modeling of the foundation by a weightless elastic material is also adopted here. An elastic-perfectly plastic model is used for the soil since it enables the development of plastic zones that may occur in the soil near the footing edges even at small service loads and it leads to more accurate solutions than a purely elastic model. For the computation of the footing displacement, the same procedure described before concerning the geostatic stresses is first used. Then, a uniform service stress is applied at the base of the footing. Finally,

damping of the system is introduced until a steady state of static equilibrium is reached in the soil.

#### 4 RELIABILITY ANALYSIS OF STRIP FOOTINGS

The aim of this paper is to perform a reliability analysis of a strip footing resting on a  $c-\phi$  soil and subjected to a vertical load. Two failure or unsatisfactory performance modes are considered in the analysis: The first one involves the ultimate limit state and emphasis on the ultimate bearing capacity of the footing and the second one considers the serviceability limit state and focuses on the maximal footing displacement. The two deterministic models presented in the previous section are used. The response surface methodology is used to find an approximation of the analytically-unknown performance functions. The cohesion  $c$ , the angle of internal friction  $\phi$ , the Young modulus  $E$  and the Poisson ratio  $\nu$  of the soil are considered as random variables. Due to the relatively low effect of the soil elastic properties on the ultimate bearing capacity, only  $c$  and  $\phi$  will be considered as random variables while studying the ultimate limit state. Similarly, only the randomness of  $E$  and  $\nu$  will be taken into consideration in the analysis of the serviceability limit state. After a brief description of the performance functions used in the present analysis, the response surface methodology and its numerical implementation are presented. Then, the probabilistic numerical results based on this method are presented and discussed.

##### 4.1 Performance functions

Two performance functions corresponding to the two unsatisfactory performance modes are used in this reliability analysis. The first one is defined with respect to the ultimate bearing capacity of the soil. It is given as follows:

$$G_1 = P_u / P_s - 1 \quad (3)$$

where  $P_u$  is the ultimate foundation load calculated using  $FLAC^{3D}$  and  $P_s$  is the footing applied load. The performance function defined with respect to a prescribed admissible footing displacement is given as follows:

$$G_2 = u_{\max} - u \quad (4)$$

where  $u$  is the vertical displacement of the footing calculated using  $FLAC^{3D}$  under a service load  $P_s$  and  $u_{\max}$  is the maximal admissible prescribed vertical displacement.

##### 4.2 Response surface method

If the performance function is an explicit function of the random variables, the reliability index can be calculated easily. In  $FLAC^{3D}$  model, the closed form solutions of the two performance functions are not available and the determination of the reliability indexes of the two limit states is then not straightforward. Therefore, an algorithm based on the response surface methodology proposed by Tandjiria et al. (2000) is used in this paper in the aim to calculate the reliability indexes and the corresponding design points. The basic idea of this method is to approximate the performance function by an explicit function of the random variables, and to improve the approximation *via* iterations. The approximate performance function used in this study has a quadratic form. It uses a second order polynomial with squared terms but no cross terms. The expression of this approximation is given by:

$$G(x) = a_0 + \sum_{i=1}^n a_i x_i + \sum_{i=1}^n b_i x_i^2 \quad (5)$$

where  $x_i$  are the random variables,  $n$  is the number of the random variables and,  $a_i$ ,  $b_i$  are the coefficients to be determined. In this paper, two random variables are considered for each limit state (*i.e.*  $n=2$ ). They are characterized by their mean values  $\mu_i$  and their coefficients of variation  $\sigma_i$ . A brief explanation of the used algorithm is as follows:

1. Evaluate the performance function  $G(x)$  at the mean value point  $\mu$  and the  $2n$  points each at  $\mu \pm k\sigma$  where  $k=1$  in this paper;
2. The above  $2n+1$  values of  $G(x)$  can be used to solve equation (5) for the coefficients ( $a_i$ ,  $b_i$ ). This obtains a tentative response surface function which is based on the values of the  $2n+1$  sampled points near the mean value point;
3. Solve equation (1) to obtain a tentative design point and a tentative  $\beta_{HL}$  subject to the constraint that the tentative response surface function of step 2 be equal to zero;
4. Repeat steps 1 to 3 until convergence. Each time step 1 is repeated, the  $2n+1$  sampled points are centred at the new tentative design point of step 3.

##### 4.3 Numerical implementation of the response surface method

As described in the previous section, the determination of the Hasofer-Lind reliability index requires (i) the determination of the coefficients ( $a_i$ ,  $b_i$ ) of the tentative response surface *via* the resolution of equation (5) for the  $2n+1$  sampled points and (ii) the minimisation of the Hasofer-Lind reliability index subject to

the constraint that the tentative response surface function of step 2 be equal to zero. These two operations which constitute a single iteration were done using the optimization toolbox available in *Matlab 7.0* software. Several iterations are performed until convergence of the reliability index.

Notice that the determination of the performance function at the  $2n + 1$  sampled points is performed using deterministic *FLAC<sup>3D</sup>* calculations. The results of these computations constitute the input data for the determination of the coefficients of the tentative response surface ( $a_i$ ,  $b_i$ ) using *Matlab 7.0*. Also, the value of the design point determined using the minimization procedure in *Matlab 7.0* is an input data for the determination of the performance function at the new  $2n + 1$  sampled points in *FLAC<sup>3D</sup>*. Therefore, an exchange of data between *FLAC<sup>3D</sup>* and *Matlab 7.0* in both directions was necessary to enable an automatic resolution of the iterative algorithm for the determination of the Hasofer-Lind reliability index. The link between *FLAC<sup>3D</sup>* and *Matlab 7.0* was performed using text files and *FISH* commands.

## 5 NUMERICAL RESULTS

For the random variables used in the ultimate limit state, different values of the coefficients of variation of the angle of internal friction and cohesion are presented in literature. The coefficient of variation of the effective angle of internal friction proposed by Phoon & Kulhawy (1999) is between 5% and 15%. For the effective cohesion, the coefficient of variation varies between 10% and 70% (Cherubini 2000). For the coefficient of correlation, Harr (1987) has shown that a correlation exists between the effective cohesion  $c$  and the effective angle of internal friction  $\varphi$ . The results of Wolff (1985) [ $\rho_{c,\varphi} = -0.47$ ] and Cherubini (2000) [ $\rho_{c,\varphi} = -0.61$ ] are among the ones cited in literature. In this paper, the illustrative values used for the statistical moments of the shear strength parameters and their coefficient of correlation are given as follows:  $\mu_c = 20$  kPa,  $\mu_\varphi = 30^\circ$ ,  $COV_c = 20\%$ ,  $COV_\varphi = 10\%$ , and  $\rho_{c,\varphi} = -0.5$ . For the probability distribution of the random variables,  $c$  is assumed to be lognormally distributed while  $\varphi$  is considered to be bounded and a Beta distribution is used (Fenton & Griffiths 2003).

For the serviceability limit state, soils with small values of Young modulus are used in this paper. In such soils, the variability of the compressibility characteristics is very large (Bauer & Pula 2000). A lognormal distribution is used for  $E$  with a mean value of 60 MPa (Nour et al. 2002). For the coefficient of variation, some values proposed and used by several authors are listed in table 1. A value of 15% is used in this paper. Regarding the Poisson ratio, there is no available information about its random variation. Some authors have

Table 1. Values of the coefficient of variation of the Young modulus proposed by several authors.

Authors	Coefficient of variation of the Young modulus (%)
Phoon and Kulhawy 1999	30
Bauer and Pula 2000	15
Nour et al. 2002	40–50
Baecher and Christian 2003	2–42

suggested that the randomness can be neglected in an analysis of settlement taking place in the case of elastic soil. Others have stated that  $\nu$  changes with a relatively narrow interval. In this paper,  $\nu$  is considered as a lognormally distributed variable with a low coefficient of variation of 5%. Its mean value is taken equal to 0.3. For the correlation coefficient of these two parameters, there is no information available. The results reported by some researchers (Bauer & Pula 2000) lead to the conclusion that this correlation is negative. In this paper, the cases of uncorrelated and correlated soil elastic properties with  $\rho_{E,\nu} = -0.5$  are considered. The threshold value of the settlement is  $u_{\max} = 0.1$  m.

It was found that for the ultimate limit state, the soil elastic properties (*i.e.*  $K$  and  $G$  or  $E$  and  $\nu$ ) have no effect on the value of the ultimate bearing capacity. Higher values of these properties,  $G = 100$  MPa and  $K = 133$  MPa (for which  $E = 240$  MPa and  $\nu = 0.2$ ), were checked. No change was observed in the value of the ultimate bearing capacity. Furthermore, a reduction by 50% in the number of cycles necessary to reach failure was noticed (*i.e.* a reduction of the computation time by half). Consequently, these values will be used in all subsequent calculations when studying the ultimate limit state.

### 5.1 Ultimate limit state

#### 5.1.1 Graphical representation of the successive tentative response surfaces

Figure 2 shows the evolution of the tentative response surfaces in the standard space ( $u_c$ ,  $u_\varphi$ ) for a footing applied load equal to 775 kN/m.

Notice that for correlated non-normal variables,  $u_c$  and  $u_\varphi$  are given by:

$$u_c = \left( \frac{c - \mu_c^N}{\sigma_c^N} \right) \quad (6)$$

$$u_\varphi = \frac{1}{\sqrt{1 - \rho_{c,\varphi}^2}} \left[ \left( \frac{\varphi - \mu_\varphi^N}{\sigma_\varphi^N} \right) - \rho_{c,\varphi} \left( \frac{c - \mu_c^N}{\sigma_c^N} \right) \right] \quad (7)$$

where  $\mu^N$  and  $\sigma^N$  are respectively the equivalent normal mean and standard deviation of the random

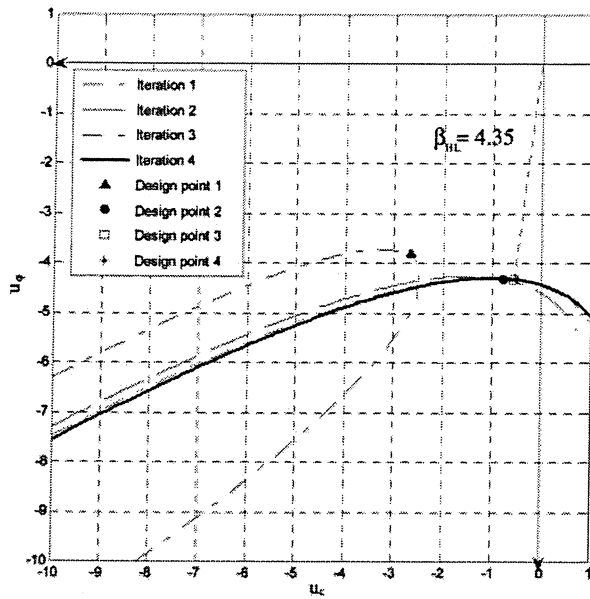


Figure 2. Evolution of the tentative response surfaces.

variables  $c$  and  $\varphi$ . A convergence criterion on the reliability index was adopted. It considers that convergence is reached when a difference smaller than  $10^{-2}$  between two successive reliability indexes is achieved. One can notice that this criterion is reached after only 4 iterations. Thus, only 20 numerical simulations using *FLAC*<sup>3D</sup> were necessary. A value of 4.35 was found for the reliability index. It should be mentioned that one can confirm the accuracy of the obtained response surface only at the design point.

### 5.1.2 Reliability index and design point

Tables 2 and 3 present the Hasofer-Lind reliability index and the corresponding design point ( $c^*$ ,  $\varphi^*$ ) for different values of the vertical applied load  $P_s$  varying from small values up to the deterministic ultimate load. Both correlated and uncorrelated shear strength parameters are considered.

The reliability index decreases with the increase of the applied load  $P_s$  (*i.e.* the decrease of the safety factor  $F = P_u/P_s$ ) until it vanishes for an applied load equal to the deterministic ultimate load. This case corresponds to a deterministic state of failure for which  $F = 1$  using the mean values of the random variables and the failure probability is equal to 50%. The comparison of the results of correlated variables with those of uncorrelated variables shows that the reliability index corresponding to uncorrelated variables is smaller than the one of negatively correlated variables. One can conclude that the hypothesis of uncorrelated shear strength parameters is conservative and non-economic in comparison to the one of negatively correlated parameters. For instance, when the safety factor is equal to 3.2 (*i.e.*  $P_s = 750$  kN/m),

Table 2. Reliability index and design point for uncorrelated shear strength parameters  $\rho_{c,\varphi} = 0$ .

$P_s$ (kN/m)	$c^*$ (kPa)	$\varphi^*$ (°)	$\beta_{HL}$	$F_c$	$F_\varphi$
750	14.12	20.86	3.49	1.42	1.52
1150	16.3	24.27	2.12	1.23	1.28
1550	17.9	26.61	1.21	1.12	1.15
1950	18.89	28.45	0.55	1.06	1.07
2394.48	20.00	30.00	0.00	1.00	1.00

Table 3. Reliability index and design point for correlated shear strength parameters  $\rho_{c,\varphi} = -0.5$ .

$P_s$ (kN/m)	$c^*$ (kPa)	$\varphi^*$ (°)	$\beta_{HL}$	$F_c$	$F_\varphi$
750	17.08	19.34	4.62	1.17	1.64
1150	18.26	23.08	2.71	1.10	1.35
1550	18.64	26.43	1.53	1.07	1.16
1950	19.92	28.14	0.67	1.004	1.08
2394.48	20.00	30.00	0.00	1.00	1.00

the reliability index increases by 32% if the variables  $c$  and  $\varphi$  are considered as negatively correlated.

The values of the design points corresponding to different values of the vertical applied load can give an idea about the partial safety factors of each of the strength parameters  $c$  and  $\tan\varphi$  as follows:

$$F_c = \frac{\mu_c}{c^*} \quad (8)$$

$$F_\varphi = \frac{\tan(\mu_\varphi)}{\tan \varphi^*} \quad (9)$$

Tables 2 and 3 show that the values of  $c^*$  and  $\varphi^*$  at the design point are smaller than their respective mean values and increase with the increase of the applied load. They tend to their mean values when the deterministic ultimate load is reached. Consequently, the partial safety factors  $F_c$  and  $F_\varphi$  decrease with the increase of the applied load. They become equal to 1 when  $P_s = P_u$ .

Contrary to the conventional codes of practice (*e.g.* Eurocode 7) which prescribe constant values of the partial safety factors, the present reliability approach has the advantage of providing different values of these factors depending on the soil variability and the value of the applied load.

### 5.1.3 Sensitivity of failure probability to the variability of the soil shear strength parameters

The failure probability of the footing under the ultimate limit state is influenced by the variability of

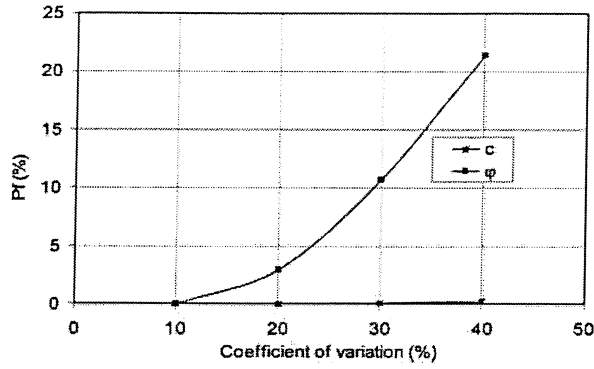


Figure 3. Effect of the variability of the soil shear strength parameters on the failure probability.

Table 4. Reliability index and design point for uncorrelated soil elastic properties  $\rho_{E,\nu} = 0$ .

$P_s$ (kN/m)	$E^*$ (MPa)	$\nu^*$	$\beta_{HL}$	$F_E$	$F_\nu$
750	19.42	0.280	7.60	3.10	1.07
1150	33.71	0.288	3.87	1.78	1.04
1550	49.75	0.296	1.21	1.21	1.01
1780	60.00	0.300	0.00	1.00	1.00

the soil shear strength parameters used in the probabilistic analysis. Since correlated variables are used in this paper, the sensitivity factors defined with respect to the transformed standard uncorrelated variables ( $\alpha_i = \delta\beta/\delta u$ ) have no physical meaning (Melchers 1999, p.101).

To study the effect of the variability of the soil shear strength on the failure probability, Figure 3 shows the failure probability versus the coefficient of variation of  $c$  and  $\phi$ . For each curve, the coefficient of variation of a parameter is hold to the same constant value given in the introduction of section 5 and the coefficient of variation of the second parameter is varied over the range 10–40%. The results show that the failure probability is highly influenced by the coefficient of variation of the angle of internal friction, the greater the scatter in  $\phi$  the higher the failure probability of the foundation. This means that the accurate determination of the distribution of this parameter is very important in obtaining reliable probabilistic results. In contrast, the coefficient of variation of  $c$  does not significantly affect the failure probability.

## 5.2 Serviceability limit state

### 5.2.1 Reliability index and design point

Tables 4 and 5 present the Hasofer-Lind reliability index and the corresponding design point ( $E^*$ ,  $\nu^*$ ) for different values of the vertical applied load  $P_s$ . Both correlated and uncorrelated soil elastic properties are considered.

Table 5. Reliability index and design point for correlated soil elastic properties  $\rho_{E,\nu} = -0.5$

$P_s$ (kN/m)	$E^*$ (MPa)	$\nu^*$	$\beta_{HL}$	$F_E$	$F_\nu$
750	16.57	0.337	8.80	3.62	0.89
1150	31.06	0.319	4.46	1.93	0.94
1550	48.37	0.306	1.41	1.24	0.98
1780	60.00	0.300	0.00	1.00	1.00

The reliability index decreases with the increase of the applied load  $P_s$ . The comparison of the results of correlated soil elastic properties with those of uncorrelated ones shows that the same conclusion drawn in the ultimate limit state remains valid here: The hypothesis of uncorrelated soil properties is conservative in comparison to the one of negatively correlated variables and leads to non-economic design. By comparing tables 4 and 5 with tables 2 and 3 respectively, one can notice that for small values of the applied load, the reliability index of the ultimate limit state is significantly smaller than that of the serviceability limit state. Thus, for small values of the applied load, the ultimate limit state is predominant and will have the highest contribution in the determination of the system failure probability. The difference between the reliability indexes of the two limit states becomes smaller for higher values of the applied load. Consequently, when the applied load increases, the two limit states (*i.e.* the ultimate and the serviceability ones) will have approximately similar contribution in the computation of the system failure probability (see more interpretation in section 5.3). The values of the design points corresponding to different values of the vertical applied load can give an idea about the partial safety factors of each of  $E$  and  $\nu$  as follows:

$$F_E = \frac{\mu_E}{E^*} \quad (10)$$

$$F_\nu = \frac{\mu_\nu}{\nu^*} \quad (11)$$

Tables 4 and 5 show that the values of  $E^*$  and  $\nu^*$  at the design point are smaller than their respective mean values and increase with the increase of the applied load. Consequently,  $F_E$  and  $F_\nu$  decrease with the increase of  $P_s$ . They become equal to 1 when  $P_s$  is equal to the load that leads to the maximal prescribed foundation settlement  $u_{\max}$  for the mean values of the soil elastic properties.

### 5.2.2 Sensitivity of failure probability to the variability of the soil elastic properties

As for the ultimate limit state, to study the effect of the variability of the soil elastic properties on the failure



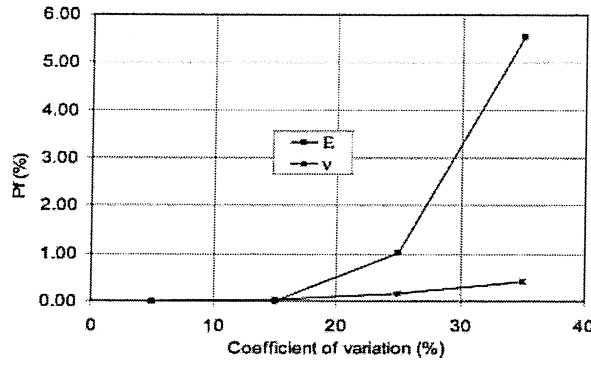


Figure 4. Effect of the variability of the soil elastic properties on the failure probability.

Table 6. System reliability index and failure probability.

$P_s$ kN/m	$\rho_{c,\varphi} = 0.0$		$\rho_{c,\varphi} = -0.5$		$\rho_{c,\varphi} = -0.5$		$\rho_{c,\varphi} = -0.0$	
	$\rho_{E,\nu} = 0.0$		$\rho_{E,\nu} = -0.5$		$\rho_{E,\nu} = -0.0$		$\rho_{E,\nu} = -0.5$	
	$\beta_{sys}$	$P_{fsys}$ (%)	$\beta_{sys}$	$P_{fsys}$ (%)	$\beta_{sys}$	$P_{fsys}$ (%)	$\beta_{sys}$	$P_{fsys}$ (%)
750	3.49	0.02	4.62	2e-4	4.62	2e-4	3.49	0.02
1150	2.12	1.70	2.71	0.34	2.70	0.34	2.12	1.70
1550	0.79	21.3	1.09	13.7	0.96	16.9	0.90	18.3

probability, Figure 4 shows the *FORM* failure probability versus the coefficient of variation of  $E$  and  $\nu$ . For each curve, the coefficient of variation of a parameter is held to the same constant value given in the introduction of section 5 and the coefficient of variation of the second parameter is varied over the range 5–35%. The results show that the failure probability of the serviceability limit state is highly influenced by the coefficient of variation of the Young modulus, the greater the scatter in  $E$  the higher the failure probability of the foundation. This means that the accurate determination of the distribution of this parameter is very important in obtaining reliable probabilistic results.

### 5.3 System failure probability

The system failure probability under the two limit states involving the ultimate and the serviceability limit states of the footing is given by:

$$P_{f,os} = P_f(U \cup S) = P_f(U) + P_f(S) - P_f(U \cap S) \quad (12)$$

where  $P_f(U \cap S)$  is the failure probability under the ultimate and the serviceability limit states and,  $P_f(U)$  is the failure probability under only the ultimate limit state and  $P_f(S)$  is the failure probability under only the serviceability limit state.

Table 6 presents the system reliability index and the corresponding failure probability for different values

of the applied load. Four cases are considered: They are the combinations of correlated and uncorrelated shear strength parameters with correlated and uncorrelated soil elastic properties. It can be shown that, even for the system reliability, the assumption of uncorrelated parameters is conservative in comparison to the one of negatively correlated variables. For small values of the applied load, where the ultimate limit state is predominant, one can notice that the system reliability index is equal to that of the ultimate limit state. When the applied load increases, the system reliability depends on both limit states and a smaller reliability index than the one corresponding to a single limit state was found. As a conclusion, both limit states have to be considered in the reliability analysis of foundations for high values of the applied load.

## 6 CONCLUSIONS

A reliability-based analysis of a strip footing resting on a  $c$ - $\varphi$  soil is presented. Both ultimate and serviceability limit states are considered. The deterministic models used are based on numerical simulations using the Lagrangian explicit finite difference code *FLAC<sup>3D</sup>*. The Hasofer-Lind reliability index is adopted here for the assessment of the foundation reliability. The response surface methodology is used to find an approximation of the analytically-unknown limit state surfaces and the corresponding reliability indexes. The main conclusions of this paper can be summarized as follows:

- The hypothesis of uncorrelated parameters was found conservative in comparison to the one of negatively correlated variables and leads to non-economic design;
- The failure probability was found highly influenced by the uncertainties of the angle of internal friction for the ultimate limit state and by the uncertainties of the Young modulus for the serviceability limit state;
- For small values of the applied load, the ultimate limit state was predominant. Consequently, the system reliability index was found equal to that of the ultimate limit state. For higher values of the applied load, the system reliability depends on both limit states and a smaller reliability index than the one corresponding to a single limit state, was found. Thus, both limit states have to be considered in the reliability analysis of foundations for high values of the applied load.

## ACKNOWLEDGMENTS

The authors would like to thank the Lebanese National Council for Scientific Research (CNRSL) and the



French organization EGIDE for providing the financial support for this research.

## REFERENCES

- Baecher, G. & Christian, J. 2003. Reliability and Statistics in Geotechnical Engineering. *Wiley*, England, 605p.
- Bauer, J. & Pula, W. 2000. Reliability with respect to settlement limit-states of shallow foundations on linearly-deformable subsoil. *Computers & Geotechnics*, 26: 281–308.
- Cherubini, C. 2000. Reliability evaluation of shallow foundation bearing capacity on  $c', \phi'$  soils. *Can. Geotech. J.*, 37:264–269.
- Fenton, G.A. & Griffiths, D.V. 2003. Bearing capacity prediction of spatially random  $c-\phi$  soils. *Can. Geotech. J.*, 40:54–65.
- Harr, M. E. 1987. Reliability-based design in civil engineering. *McGraw-Hill Book Company*, New York, 290p.
- Hasofer, A. M. & Lind, N. C. 1974. Exact and invariant second-moment code format. *J. of Engrg. Mech.*, ASCE, 100(1):11–121.
- Low, B. K. 2005. Reliability-based design applied to retaining walls. *Géotechnique*, 55(1):63–75.
- Low, B. K. & Tang, W. H. 1997. Efficient reliability evaluation using spreadsheet. *J. of Engrg. Mech.*, ASCE, 123: 749–752.
- Melchers, R. 1999. Structural reliability analysis and prediction. *Wiley*, England, 437p.
- Nour, A., Slimani, A. & Laouami N. 2002. Foundation settlement statistics via finite element analysis. *Computers & Geotechnics*, 29:641–672.
- Phoon, K.-K. & Kulhawy, F.H. 1999. Evaluation of geotechnical property variability. *Can. Geotech. J.*, 36:625–639.
- Tandjiria, V., Teh, C.I. & Low, B.K. 2000. Reliability analysis of laterally loaded piles using response surface methods. *Structural Safety*, 22:335–355.
- Wolff, T. H. 1985. Analysis and design of embankment dam slopes: A probabilistic approach. Ph.D. thesis, *Purdue University*, Lafayette, Ind.
- Yin, J.-H., Wang, Y.-J. & Selvadurai, P.S. 2001. Influence of nonassociativity on the bearing capacity of a strip footing. *J. of Geotech. & Geoenv. Engrg.*, ASCE, 127(11): 985–989.
- Youssef Abdel Massih, D.S., Soubra, A.-H. & Low, B.K. 2007. Reliability-based analysis and design of strip footings against bearing capacity failure. *J. of Geotech. & Geoenv. Engrg.*, ASCE, under review.